Engineering Fracture Mechanics Vol. 26, No. 5, pp. 691–700, 1987.
Printed in Great Britain

0013–7944/87 $3.00 + .00
Pergamon Journals Ltd.

# AN IMPROVED METHOD FOR COMPUTING THE $J_2$ INTEGRAL

J. W. EISCHEN†
Department of Mechanical and Aerospace Engineering, North Carolina State University, Raleigh, NC 27695, U.S.A.

**Abstract**—The $J_2$ integral, used in conjunction with the well-known $J$ (or $J_1$) integral, can assist the analyst in the prediction of in-plane mixed-mode stress intensity factors via finite element stress analysis. However, direct evaluation of $J_2$ yields results which are very sensitive to the crack tip modeling employed, thus reducing the efficacy of the $J_2$ integral. A new technique is proposed to circumvent this problem. This new technique also permits one to easily calculate the non-singular stress component $\sigma_{x0}$, which is known to be important in predicting crack kinking angles.

## 1. INTRODUCTION

THE SUBJECT of the $J_k(k=1,2)$ path-independent integrals of fracture mechanics has received considerable attention from researchers with regard to numerical determination of mixed-mode stress intensity factors. A recent article by Nishioka[1] described a procedure allowing separation of the stress intensity factors for an arbitrarily shaped cracked body via finite element analysis. It was discovered that in order to employ the $J_k$ integrals directly, it is necessary to accurately model the crack tip region with elements which possess the $r^{-1/2}$ strain singularity known to exist at a sharp crack tip, and failure to use such elements results in substantially inaccurate values for the stress intensity factors.

The primary aim of this paper is to illustrate how the $J_k$ integrals can be used directly to produce accurate results when the crack tip region is not modeled with singular elements. It will also be shown that the so-called non-singular stress component $\sigma_{x0}$, known to influence crack kinking angles[2], can be obtained by considering a new quantity called $\hat{J}_2$.

As an aside, the path-independence of the $J_2$ integral has been a recent topic of discussion. In a paper by Herrmann[3] the path independence of $J_2$ was addressed for a center-cracked plate geometry, and it was stated that $J_2$ is path-dependent for paths surrounding the crack tip. Path-dependency in this is shown to be the sole consequence of the definition of $J_2$. If $J_2$ is defined in a manner consistent with $J_1$, path independence is assured.

The paper is organized as follows. First, the $J_k$ integrals are derived from a conservation law of linear elasticity theory and their path-independence property is established. Subsequently, an approximate expression for $J_2$ is proposed in order to facilitate numerical computations. Finally, the viability of the proposed procedure for separating mixed mode stress intensity factors and determining the non-singular stress component is illustrated with the aid of a numerical example.

## 2. CONSERVATION LAW

Consider a two-dimensional deformation field described by the displacement components $u_i=u_i(x_1,x_2)$‡, where $x_1$ and $x_2$ are Cartesian coordinates. The strain energy density $W$ for an elastic, homogeneous material is defined by

$$W = W(\varepsilon_{ij}) \equiv \int_0^{\varepsilon_{ij}} \sigma_{mn} d\varepsilon_{mn} \tag{1}$$

† Assistant Professor.
‡ Subscripts have the range 1–2; a subscript preceeded by a comma indicates partial differentiation, and summation over repeated indices is implied.

where $\sigma_{ij}$ are components of the stress tensor, and $\varepsilon_{ij}$ are components of the infinitesimal strain tensor. Conservation laws in elasticity can be derived in a number of ways. For the present purpose a direct approach is followed, which begins by forming the gradient of $W$

$$\nabla W = \frac{\partial W}{\partial x_k} = \frac{\partial W}{\partial \varepsilon_{ij}} \frac{\partial \varepsilon_{ij}}{\partial x_k}. \tag{2}$$

Recognizing that

$$\sigma_{ij} = \frac{\partial W}{\partial \varepsilon_{ij}} \tag{3}$$

eq. (2) becomes

$$\frac{\partial W}{\partial x_k} = \sigma_{ij} \frac{\partial \varepsilon_{ij}}{\partial x_k}. \tag{4}$$

Using the linearized strain–displacement relations, the symmetry properties of the stress tensor, the equilibrium equations, and converting to indicial notation, eq. (4) can be written as

$$(W\delta_{jk} - \sigma_{ij}u_{i,k})_{,j} = 0. \tag{5}$$

This expression represents a *conservation law* for a homogeneous, elastic body, free of body forces. The Kronecker delta is indicated by $\delta_{jk}$. An integral form of eq. (5) is obtained by applying the divergence theorem, resulting in

$$\int_{\Gamma} (Wn_k - \sigma_{ij}n_j u_{i,k}) \, d\Gamma = 0 \tag{6}$$

where $\Gamma$ is any closed curve in the $x_1$, $x_2$ plane that encloses no defects, cracks, or material nonhomogeneities. The measure numbers of the outward unit normal vector to $\Gamma$ are denoted by $n_j$.

## 3. PATH-INDEPENDENCE OF $J_k$ INTEGRALS

Figure 1 shows a cracked body whose boundary is subjected to applied tractions and specified displacement boundary conditions. A path $\Gamma$ composed of segments $\Gamma_0$, $\Gamma_c^+$, $\Gamma_c^-$, and $\Gamma_\varepsilon$ is also shown. The region inside $\Gamma$ excludes the crack tip, and therefore eq. (6) holds such that

$$\int_{\Gamma_0} (Wn_k - \sigma_{ij}n_j u_{i,k}) \, d\Gamma + \delta_{k2} \int_{\Gamma_c} [W^+ - W^-] n_2^+ \, d\Gamma = \int_{\Gamma_\varepsilon} (Wn_k - \sigma_{ij}n_j u_{i,k}) \, d\Gamma \tag{7}$$

where $W^+$ and $W^-$ indicate the magnitude of the strain energy density on the top and bottom crack surfaces, respectively. The notation $[W^+ - W^-]$ denotes a discontinuity (or "jump") in the strain energy density across the crack opening. The integrals along $\Gamma_c^+$ and $\Gamma_c^-$ have been combined into one term, with the associated path of integration simply called $\Gamma_c$. Crack surfaces are assumed traction-free. The vector $J_k$ is then defined according to

$$J_k \equiv \lim_{\Gamma_\varepsilon \to 0} \int_{\Gamma_\varepsilon} (Wn_k - \sigma_{ij}n_j u_{i,k}) \, d\Gamma. \tag{8}$$

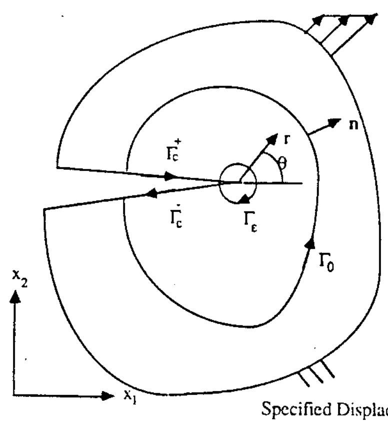


Fig. 1 Cracked body and integration paths for $J_k$ integrals.

If the general expressions for the elastic stress and displacement fields near a crack tip are used in eq. (8), one finds

$$J_1 = \frac{K_I^2 + K_{II}^2}{E} \tag{9}$$

$$J_2 = \frac{-2K_I K_{II}}{E} \tag{10}$$

for plane stress. For plane strain, Young's modulus $E$ must be divided by $(1 - \nu^2)$, where $\nu$ is Poisson's ratio. $K_I$ and $K_{II}$ are the Mode I and Mode II stress intensity factors, respectively. From eqs (7) and (8), it follows that

$$J_1 = \int_{\Gamma_0} (Wn_1 - \sigma_{ij} n_j u_{i,1})\, d\Gamma = \frac{K_I^2 + K_{II}^2}{E} \tag{11}$$

$$J_2 = \int_{\Gamma_0} (Wn_2 - \sigma_{ij} n_j u_{i,2})\, d\Gamma + \int_{\Gamma_c} [W^+ - W^-] n_2^+\, d\Gamma = \frac{-2K_I K_{II}}{E}\,. \tag{12}$$

These expression for $J_1$ and $J_2$ are path-independent. The path $\Gamma_0$ can trace any curve in the $x_1 - x_2$ plane which begins on the lower crack face and ends on the upper crack face. Budiansky[4] did not include the integration along $\Gamma_c$ in defining $J_2$. This omission clearly leads to path-*dependence* for the $J_2$ integral. Herrmann[3] verified this discrepancy for a specific crack geometry (center-cracked plate with uniform remote loading), but did not address the issue in the context of general loadings acting on arbitrarily shaped cracked bodies.

## 4. EVALUATION OF THE $J_2$ INTEGRAL

The expression for $J_2$ given by eq. (12) includes an integration along the crack face of the discontinuity in the strain energy density, while the expression for $J_1$ does not. This term causes difficulty in numerical evaluation of $J_2$. It is useful to derive an expression for $[W^+ - W^-]$ near a crack tip. The expressions for the stresses near a crack tip were given by Eftis *et al.*

$$\sigma_{11} = \frac{K_I}{\sqrt{2\pi r}} f_{11}^{I}(\theta) + \frac{K_{II}}{\sqrt{2\pi r}} f_{11}^{II}(\theta) + \sigma_{x0} + O(r^{1/2}) + \ldots \tag{13}$$

$$\sigma_{22} = \frac{K_I}{\sqrt{2\pi r}} f_{22}^{I}(\theta) + \frac{K_{II}}{\sqrt{2\pi r}} f_{22}^{II}(\theta) + O(r^{1/2}) + \ldots \tag{14}$$

$$\sigma_{12} = \frac{K_I}{\sqrt{2\pi r}} f_{12}^{I}(\theta) + \frac{K_{II}}{\sqrt{2\pi r}} f_{12}^{II}(\theta) + O(r^{1/2}) + \ldots \tag{15}$$

where $r, \theta$ are polar coordinates with origin at the crack tip, as shown in Fig. 1. The symbols $f_{ij}^{I,II}(\theta)$ represent simple trigonometric functions of the angle $\theta$, and are given explicitly by Eftis *et al.*[5]. The notation $O(r^{1/2})$ reads "order $r^{1/2}$" and indicates a term proportional to $r^{1/2}$. The ellipses indicate a sequence of terms of successively higher degree in $r$. The so-called "non-singular" stress $\sigma_{x0}$ depends on the geometry of the cracked body and the imposed loading, as do the stress intensity factors. The $\sigma_{x0}$ contribution to $\sigma_{11}$ is commonly neglected in comparison with the singular terms, but as will be seen, its contribution is crucial to a correct computation of the $J_2$ integral. Recalling that for plane stress

$$W = \frac{1}{2E}(\sigma_{11}^2 + \sigma_{22}^2 - 2\nu\sigma_{11}\sigma_{22}) + \frac{1+\nu}{E}\sigma_{12}^2. \tag{16}$$

Substituting eqs (13)–(15) in eq. (16) and performing some simple manipulations yields

$$W(r,\pi) - W(r,-\pi) = [W^+ - W^-] = \frac{-4K_{II}\sigma_{x0}}{E\sqrt{2\pi r}} + O(r^{1/2}) + \ldots \tag{17}$$

While the singularity in the strain energy density near a crack tip is proportional to $1/r$, the singularity in the discontinuity of the strain energy density is proportional to $1/\sqrt{r}$. The spatial dependence of $[W^+ - W^-]$ near a crack tip does not vary from one crack problem to another. The only quantity which does vary is the product $K_{II}\sigma_{x0}$, as shown in eq. (17). This universal spatial dependence is analogous to the universal spatial dependence exhibited by the stress and displacement fields near a crack tip.

The next issue to be considered is the evaluation of the $J_2$ integral using knowledge of the form of $[W^+ - W^-]$ near the crack tip. This discussion is conducted assuming that a numerical determination (e.g. finite elements) of $J_2$ will be made. The first term in eq. (12) involves a line integral on the curve $\Gamma_0$, and is typically evaluated very accurately by numerical analysis methods because the crack tip region is avoided. However, the second term in eq. (12) involves an integration along the crack face including the crack tip region and accurate results are difficult to obtain unless a very fine mesh and/or singular elements are utilized. The use of the explicit form of $[W^+ - W^-]$ valid near the crack tip will be shown to aid in evaluating this term.

For reasons which will soon become clear, the range of integration along the crack face is split into two parts, the first part remote from the crack tip, and the second part in close proximity to the crack tip. Consequently, a characteristic distance from the crack tip is introduced, denoted $\delta$, as shown in Fig. 2. Henceforth, the origin of the $x_1$ axis will located at the point where the path $\Gamma_0$ intersects the crack face. The distance from this point to the crack tip is $d$. It will be assumed that over the distance $\delta$, $[W^+ - W^-]$ is sufficiently approximated by the asymptotic form $-4K_{II}\sigma_{x0}/E\sqrt{2\pi r}$. The following approximation is made to the integration of $[W^+ - W^-]$ along the crack face

$$\int_{\Gamma_c}[W^+ - W^-]n_2^+\,d\Gamma = -[W^+ - W^-]\,dx_1 \approx -\int_0^{d-\delta}[W^+ - W^-]\,dx_1 - \int_{d-\delta}^{d}\frac{-4K_{II}\sigma_{x0}}{E\sqrt{2\pi r}}\,dx_1. \tag{18}$$

Making use of the fact that along the crack face $r = d - x_1$, the last integral in eq. (18) can be evaluated explicitly to give

$$\int_{\Gamma_c}[W^+ - W^-]n_2^+\,d\Gamma \approx -\int_0^{d-\delta}[W^+ - W^-]\,dx_1 + \frac{8K_{II}\sigma_{x0}\delta^{1/2}}{E\sqrt{2\pi}}. \tag{19}$$

In summary, the approximate expression for $J_2$ is then

$$J_2 \approx \int_{\Gamma_0}(Wn_2 - \sigma_{ij}n_j u_{i,2})\,d\Gamma - \int_0^{d-\delta}[W^+ - W^-]\,dx_1 + \frac{8K_{II}\sigma_{x0}\delta^{1/2}}{E\sqrt{2\pi}}. \tag{20}$$

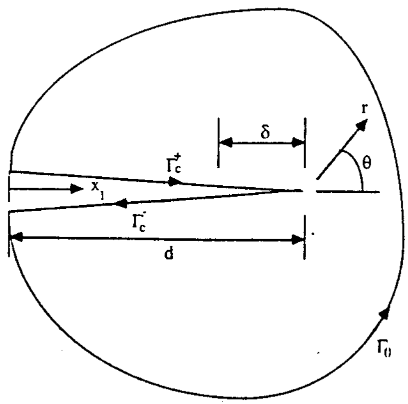


Fig. 2 Schematic of integration path used along crack face.

The next section of the paper presents an analysis showing how large $\delta$ can be with respect to $d$ for eq. (19) to represent a reasonable approximation to the $J_2$ integral.

## 5. ANALYTICAL APPRAISAL OF THE APPROXIMATE $J_2$ INTEGRAL

The often studied center-cracked sheet geometry provides a useful example to assess the accuracy of the approximate $J_2$ given by eq. (20), because exact analytical expressions for the stresses and displacements are available. Figure 3 shows the configuration and the imposed remotely applied loading. The sheet contains a through crack of length $2a$ and is subjected to far field stresses $\sigma_{11}^A$, $\sigma_{22}^A$, and $\sigma_{12}^A$. The well known expressions for the stress intensity factors are shown in Fig. 3. The non-singular stress component $\sigma_{xo}$ is equal to $\sigma_{11}^A - \sigma_{22}^A$. This result can be obtained from the complex potential form of the solution to this problem[5].

The term $[W^+ - W^-]$, valid over the entire crack face, is given by Herrman[3] in closed form as

$$[W^+ - W^-] = \frac{-4\sigma_{12}^A(\sigma_{11}^A - \sigma_{22}^A)}{E} \frac{x_1}{(a^2 - x_1^2)^{1/2}}. \tag{21}$$

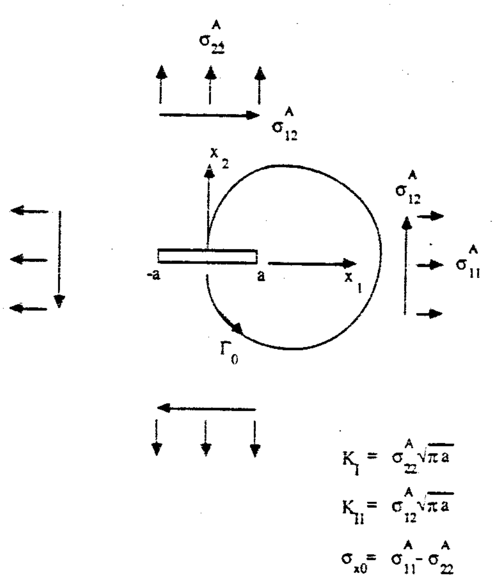


Fig. 3 Configuration of center-cracked plate geometry.

Table 1

| $\alpha = \delta/a$ | $f(\alpha)$ |
|---|---|
| 0.00 | 1.00 |
| 0.10 | 1.01 |
| 0.20 | 1.03 |
| 0.30 | 1.06 |
| 0.40 | 1.09 |
| 0.50 | 1.13 |
| 0.60 | 1.18 |
| 0.70 | 1.23 |
| 0.80 | 1.29 |
| 0.90 | 1.35 |
| 1.00 | 1.41 |

The contribution to $J_2$ from the strain energy density discontinuity can be obtained exactly by employing eq. (21) in eq. (12). The path $\Gamma_0$ is assumed to cross the $x_1$-axis at $x_1 = 0$. Therefore,

$$\int_{\Gamma_c} [W^+ - W^-] n_2^+ \, d\Gamma = \int_0^a \frac{4\sigma_{12}^A \sigma_{11}^A - \sigma_{22}^A}{E} \frac{x_1}{(a^2 - x_1^2)^{1/2}} \, dx_1 = \frac{4K_{II}\sigma_{x0}\sqrt{a}}{E\sqrt{\pi}}. \tag{22}$$

The approximate expression for this term, given by eq. (19), can then be evaluated by letting $d = a$

$$\begin{aligned} \int_{\Gamma_c} [W^+ - W^-] n_2^+ \, d\Gamma &\approx -\int_0^{a-\delta} [W^+ - W^-] \, dx_1 + \frac{8K_{II}\sigma_{x0}\delta^{1/2}}{E\sqrt{\pi}} \\ &= \frac{-4K_{II}\sigma_{x0}}{E\sqrt{\pi a}} [(2a\delta - \delta^2)^{1/2} - a] + \frac{8K_{II}\sigma_{x0}\delta^{1/2}}{E\sqrt{2\pi}}. \end{aligned} \tag{23}$$

Letting $\delta = \alpha a$, where $0 < \alpha < 1$, eq. (23) becomes

$$\int_{\Gamma_c} [W^+ - W^-] n \, d\Gamma \approx \frac{4K_{II}\sigma_{x0}\sqrt{a}}{E\sqrt{\pi}} \quad [1 - (2\alpha - \alpha^2)^{1/2} + (2\alpha)^{1/2}]. \tag{24}$$

The function $f(\alpha)$ is introduced as

$$f(\alpha) = 1 - (2\alpha - \alpha^2)^{1/2} + (2\alpha)^{1/2}. \tag{25}$$

Comparing eqs (22) and (24), it is apparent that $f(\alpha)$ provides a measure of the error introduced by using the asymptotic form of $[W^+ + W^-]$ over a region of the crack face near the crack tip. Table 1 shows $f(\alpha)$ versus $\alpha$. Examination of Table 1 reveals that the distance $\delta$ can be a substantial fraction of the half crack length $a$ before the approximate expression for

$$\int_{\Gamma_c} [W^+ - W^-] n_2^+ \, d\Gamma$$

produces inaccurate results. For example, $\delta$ can be 40% of the half crack length, and the approximate expression for $J_2$ is valid to within 10%. This fact bodes well for numerical stress analysis because the integration for the strain energy discontinuity term can stay well away from the crack tip, where errors in the field quantities may be expected, especially when standard finite elements are used.

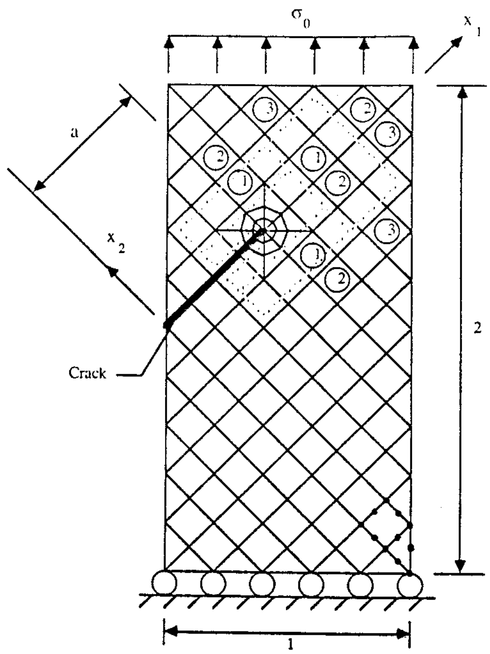


Fig. 4 Finite element mesh used for example problem.

## 6. NUMERICAL PROCEDURE

The utility of the approximation to the $J_2$ integral is most obvious when numerical computations are performed. In order to compute mixed-mode stress intensity factors, both the $J_1$ and $J_2$ integrals must be calculated. The integrations are performed on paths $\Gamma^i = \Gamma_0^i + \Gamma_c^i$ which surround a single crack tip, as shown in Fig. 4. The superscript $i$ refers to the path under consideration. Evaluations of $J_1$ and $J_2$ are typically conducted on multiple paths in order to verify path-independence, thereby providing a check on the numerical consistency of the results.

A local Cartesian coordinate system with axes $x_1$, $x_2$ is established such that the $x_1$ axis is aligned with the crack faces, and the origin is located at the point where the paths $\Gamma_0^i$ intersect the crack faces. The $J_1$ integral evaluation involves only the paths $\Gamma_0^i$, since no integration on the crack faces is required, unless crack face tractions are present. The paths $\Gamma_0^i$ are assumed to follow element boundaries. The stress and displacement gradient quantities needed to evaluate $J_1$ are computed at the Gauss integration points on element interiors. A local smoothing algorithm described by Hinton[6] is then exercised to produce the required quantities on the element boundaries. The numerical value of the $J_1$ integral is related to the stress intensity factors according to eq. (9). The $J_2$ integral requires evaluations of the stress and displacement gradient quantities on the $\Gamma_0^i$ paths, as well as the strain energy density discontinuity along the upper and lower crack faces ($\Gamma_c^i$). If the crack faces are traction free, a very simple expression for the strain energy density emanates

$$\begin{aligned} W &= \frac{1}{2}\sigma_{11}\varepsilon_{11} \\ &= \frac{1}{2}E\varepsilon_{11}^2 \quad \text{(plane stress)}. \end{aligned} \tag{27}$$

The strain quantity $\varepsilon_{11}$ is evaluated directly on the crack faces, rather than being smoothed from the element interiors.

The quantity $\hat{J}_2$ is then introduced as

$$\hat{J}_2 = \int_{\Gamma_0^i} (Wn_2 - \sigma_{ij}n_y u_{i,2})\,\mathrm{d}\Gamma - \int_0^{d-\delta} [W^+ - W^-]\,\mathrm{d}x_1. \tag{28}$$

Upon examining eqs (10) and (20), it follows that

$$\hat{J}_2 = -\frac{2K_IK_{II}}{E} - \frac{8K_{II}\sigma_{x0}}{E\sqrt{2\pi}}\sigma^{1/2}. \tag{29}$$

The quantity $\hat{J}_2$ is computed numerically on each path $\Gamma^i = \Gamma_0^i + \Gamma_c^i$, using eq. (28), for two values of $\delta(\delta_1$ and $\delta_2)$. These values of $\hat{J}_2$ are called $\hat{J}_2^n$, $n = 1,2$. Therefore

$$\hat{J}_2^1 = -\frac{2K_IK_{II}}{E} - \frac{8K_{II}\sigma_{x0}}{E\sqrt{2\pi}}\delta_1^{1/2} \tag{30}$$

$$\hat{J}_2^2 = -\frac{2K_IK_{II}}{E} - \frac{8K_{II}\sigma_{x0}}{E\sqrt{2\pi}}\delta_2^{1/2} \tag{31}$$

Once $J_1$, $\hat{J}_2^1$, and $\hat{J}_2^2$ have been computed numerically, eqs (9), (30)–(31) can be solved for $K_I$, $K_{II}$, and $\sigma_{xo}$. The solution is accomplished as follows. Equations (30) and (31) are solved to give

$$-\frac{2K_IK_{II}}{E} = J_2 = \frac{\hat{J}_2^1\delta_2^{1/2} - \hat{J}_2^2\delta_1^{1/2}}{\delta_2^{1/2} - \delta_1^{1/2}} \tag{32}$$

$$-\frac{8K_{II}\sigma_{x0}}{E\sqrt{2\pi}} = S = \frac{\hat{J}_2^2 - \hat{J}_2^1}{\delta_2^{1/2} - \delta_1^{1/2}} \tag{33}$$

Then

$$K_I = \pm\left\{\frac{EJ_1}{2}\left[1 \pm \left(1 - \left(\frac{J_2}{J_1}\right)^2\right)^{1/2}\right]\right\}^{1/2} \tag{34}$$

$$K_{II} = \pm\left\{\frac{EJ_1}{2}\left[1 \mp \left(1 - \left(\frac{J_2}{J_1}\right)^2\right)^{1/2}\right]\right\}^{1/2} \tag{35}$$

The signs of $K_I$ and $K_{II}$ are determined by monitoring the magnitudes of the crack opening displacements near the crack tip. The crack opening displacments are defined by

$$\Delta_I = u_2^+ - u_2^- \qquad \Gamma_{II} = u_1^+ - u_1^- \tag{36}$$

where the $()^+$ and $()^-$ refer to the upper and lower crack faces, respectively. The signs of $K_I$ and $K_{II}$ correspond to the signs of $\Delta_I$ and $\Delta_{II}$, respectively (i.e. if $\Delta_I > 0$, $K_I > 0$, etc.). The sign of the term in the braces [ ] of eqs (34) and (35) is determined by checking

$$\text{if } |\Delta_I| \geqslant |\Delta_{II}| \quad \text{take } [+] \tag{37}$$

$$\text{if } |\Delta_I| < |\Delta_{II}| \quad \text{take } [-] \tag{38}$$

Finally

$$\sigma_{xo} = -\frac{\sqrt{2\pi}ES}{8K_{II}} \tag{39}$$

The feasibility of the procedure explained above is illustrated in the following section by means of a numerical example.

## 7. NUMERICAL RESULTS

The slanted crack in a finite two-dimensional elastic plate provides a mixed-mode loading situation which is useful for checking new numerical procedures which separate stress intensity factors. Figure 4 shows the geometry, loading and boundary conditions for the problem selected to serve as an example. This configuration is nearly identical to the one solved by Nishioka[1]. Three integration paths are also shown ($\Gamma_0^i$, $i = 1,2,3$). Eight node Serendipity quadrilateral elements

Table 2
Stress intensity factors and $\sigma_{x0}$ computed by new procedure

| Crack tip elements | $K_I/\sigma_0\sqrt{\pi a}$ | $K_{II}/\sigma_0\sqrt{\pi a}$ | $\sigma_{x0}/\sigma_0$ |
|---|---|---|---|
| Singular | 1.438 | 0.605 | 0.822 |
| Non/singular | 1.410 | 0.625 | 0.621 |
| Bowie[7] | 1.450 | 0.620 | N.A. |

were used over most the mesh, while near the crack tip two element types were employed; (i) quarter-point, singular, isoparametric, six-node triangles, (ii) non-singular, isoparametric, six-node triangles. It should be noted that the first element type correctly captures the $1/\sqrt{r}$ strain singularity known to exist at the crack tip. The values of the parameter $\delta$ chosen for this analysis were $a/12$ and $a/6$. This meant terminating the integration along the crack face either one or two elements from the crack tip, respectively. The normalized values computed for $K_I$, $K_{II}$, and $\sigma_{x0}$ using the new procedure outlined above, whereby $J_1$ and $\hat{J}_2$ are employed, are shown in Table 2.

The results Bowie[7] reported for this problem were obtained using a highly accurate mapping technique. The present results for the stress intensity factors are seen to agree very well with Bowie's results, independent of the crack tip modeling. Results have not been reported before for the $\sigma_{x0}$ stress component. Results for $\sigma_{x0}$ reported here are somewhat sensitive to the crack tip modeling. Crack curving criteria predict that the crack will kink in the presence of a positive value of $\sigma_{x0}$. The positive value computed numerically (0.621–0.822) indicates imminent crack kinking, which certainly would be expected given the loading and geometry considered.

The values computed for $K_I$, $K_{II}$, and $\sigma_{x0}$ using the standard procedure, whereby $J_1$ and $J_2$ are computed directly, are shown in Table 3. In the standard procedure, the integration along the crack face of $[W^+ - W^+]$ proceeds all the way into the crack tip. These results illustrate the extreme sensitivity of the computation to the crack tip modeling. The value of $K_{II}$ is computed very inaccurately when non-singular elements are present at the crack tip. These results are consistent with those reported by Nishioka[1]. Also, the standard procedure does not allow determination of the non-singular stress component.

The stress intensity factors and $\sigma_{x0}$ were also computed by examining the displacement components $u_1$ and $u_2$ near the crack tip. The series solutions for the displacements near a crack tip were used in combination with linear regression analysis to extract $K_I$, $K_{II}$, and $\sigma_{x0}$. Terms proportional to $r^0$, $r^{1/2}$, $r^1$, and $r^{3/2}$ were retained in the series for purpose of the regression analysis. Terms $O(r^{5/2})$ and above were neglected. These results are presented in Table 4, and are seen to be generally consistent with those presented above.

## 8. CONCLUDING REMARKS

A path-independent form of the $J_2$ integral has been generated and then used in conjunction with $J$ to compute mixed-mode stress intensity factors. A new quantity called $\hat{J}_2$, when used together with $\hat{J}_2$ is shown to contain information regarding the non-singular stress component $\sigma_{x0}$. The new procedure described in this paper allows computation of in-plane mixed-mode stress intensity factors without the need for detailed crack tip modeling.

Table 3
Stress intensity factors and $\sigma_{x0}$ computed by new procedure

| Crack tip elements | $K_I/\sigma_0\sqrt{\pi a}$ | $K_{II}/\sigma_0\sqrt{\pi a}$ | $\sigma_{x0}/\sigma_0$ |
|---|---|---|---|
| Singular | 1.438 | 0.602 | N.A. |
| Non/singular | 1.410 | 0.394 | N.A. |
| Bowie[7] | 1.450 | 0.620 | N.A. |

Table 4
Stress intensity factors and $\sigma_{x0}$ computed from near tip displacements (singular elements)

| Crack tip elements | $K_I/\sigma_0\sqrt{\pi a}$ | $K_{II}/\sigma_0\sqrt{\pi a}$ | $\sigma_{x0}/\sigma_0$ |
|---|---|---|---|
| $u_1$ Regression | 1.437 | 0.613 | 0.783 |
| $u_2$ Regression | 1.410 | 0.625 | 0.621 |
| Bowie[7] | 1.438 | 0.620 | N.A. |

*Acknowledgement*—Financial support provided by the Shell Foundation Teaching Fellowship to Standford University is gratefully acknowledged.

## REFERENCES

[1] T. Nishika and S. N. Atluri, On the computation of mixed-mode k-factors for a dynamically propagating crack using path-independent integrals. *Engng Fracture Mech.* **20,** 193–208 (1984).
[2] M. Ramulu and A. S. Kobayashi, Strain energy density fracture criteria in elastodynamic mixed mode crack propagation. Office of Naval Research, Technical Report No. UWA/DME/TR-82/44, (1982).
[3] A. G. Herrmann and G. Herrmann, On energy release rates for a plane crack, *J. appl. Mech.* **48,** 525–528 (1981).
[4] B. Budiansky and J. R. Rice, Conservation laws and energy-release rates, *J. appl. Mech* **40,** 201–203 (1973).
[5] J. Eftis, N. Subramonian and H. Liebowitz, Crack border stress and displacement equations revisited, *Engng Fracture Mech* **9,** 189–210 (1977).
[6] E. Hinton and J. S. Campbell, Local and global smoothing of discontinuous finite element functions using a least squares method. *Int. J. numer. Meth. Engng* **8,** 461–480 (1974).
[7] O. L. Bowie, Solution of crack problems by mopping technique, *Mechanics of Fracture I*, pp. 1–55, Noordhoff (1973).

(*Received* 13 *May* 1986)